Tensional homeostasis and the malignant phenotype

Matthew J. Paszek,[1,2,6] Nastaran Zahir,[1,2,6] Kandice R. Johnson,[1,2] Johnathon N. Lakins,[2] Gabriela I. Rozenberg,[2] Amit Gefen,[3] Cynthia A. Reinhart-King,[1] Susan S. Margulies,[1] Micah Dembo,[4] David Boettiger,[5] Daniel A. Hammer,[1] and Valerie M. Weaver[2,*]

[1]Department of Bioengineering, University of Pennsylvania, Philadelphia, Pennsylvania 19104
[2]Department of Pathology and Institute for Medicine and Engineering, University of Pennsylvania, Philadelphia, Pennsylvania 19104
[3]Department of Biomedical Engineering, Tel Aviv University, Tel Aviv 69978, Israel
[4]Department of Biomedical Engineering, Boston University, Boston, Massachusetts 02215
[5]Department of Microbiology, University of Pennsylvania, Philadelphia, Pennsylvania 19104
[6]These authors contributed equally to this work.
*Correspondence: vmweaver@mail.med.upenn.edu

Summary

Tumors are stiffer than normal tissue, and tumors have altered integrins. Because integrins are mechanotransducers that regulate cell fate, we asked whether tissue stiffness could promote malignant behavior by modulating integrins. We found that tumors are rigid because they have a stiff stroma and elevated Rho-dependent cytoskeletal tension that drives focal adhesions, disrupts adherens junctions, perturbs tissue polarity, enhances growth, and hinders lumen formation. Matrix stiffness perturbs epithelial morphogenesis by clustering integrins to enhance ERK activation and increase ROCK-generated contractility and focal adhesions. Contractile, EGF-transformed epithelia with elevated ERK and Rho activity could be phenotypically reverted to tissues lacking focal adhesions if Rho-generated contractility or ERK activity was decreased. Thus, ERK and Rho constitute part of an integrated mechanoregulatory circuit linking matrix stiffness to cytoskeletal tension through integrins to regulate tissue phenotype.

Introduction

Tumors are frequently detected through physical palpation as a rigid mass residing within a compliant tissue. Indeed, screening for tumors by monitoring for tissue stiffness is widespread, and strategies to image differences in tissue compliance have been exploited for cancer screening (Khaled et al., 2004). Although patients with fibrotic "stiff" lesions have a poor prognosis (Colpaert et al., 2001), the relationship between tissue rigidity and tumor behavior at the molecular level is unclear.

Tumor rigidity likely reflects an elevation in interstitial tissue pressure and solid stress due to a perturbed vasculature and tumor expansion (Padera et al., 2004), an increase in the elastic modulus of transformed cells mediated by an altered cytoarchitecture (Beil et al., 2003), and matrix stiffening linked to fibrosis (Paszek and Weaver, 2004). Tumor rigidity could influence treatment efficacy (Netti et al., 2000) and may enhance tumor metastasis (Akiri et al., 2003). Whether tissue stiffness could actively promote malignant transformation—and how it could do so—have yet to be assessed.

Extracellular matrix (ECM) orientation mediates tension-dependent cell migration to orchestrate developmental processes such as gastrulation (Keller et al., 2003), and matrix rigidity influences cell growth, viability, differentiation, and motility (Engler et al., 2004; Lo et al., 2000; Yeung et al., 2005). Matrix compliance influences cell contractility (cytoskeletal tension), Rho activity, and ERK-dependent growth (Wang et al., 1998; Wozniak et al., 2003), and cytoskeletal tension promotes growth (Roovers and Assoian, 2003) and focal adhesion (FA) assembly (Burridge and Wennerberg, 2004). This suggests that cell behavior, matrix stiffness, Rho, and cell contractility are functionally linked. Consistently, Rho-dependent cytoskeletal tension is implicated in branching morphogenesis (Moore et al., 2002), and ROCK disrupts adherens junctions (AJs) (Sahai and Marshall, 2002). Three-dimensional (3D) culture studies emphasize the importance of matrix compliance for normal tissue differentiation (Paszek and Weaver, 2004) and imply that matrix stiffness regulates cell fate by modulating growth factor (GF) signaling and Rho GTPase function (O'Brien et al., 2001; Wang et al., 1998). Indeed, Rho activity is often elevated in

SIGNIFICANCE

By examining the significance of the relationship between tissue rigidity and tumor behavior at the molecular level, we showed that tissue rigidity reflects matrix stiffening and elevated Rho GTPase-dependent cytoskeletal tension. We found that matrix stiffness (exogenous force) and cytoskeletal tension (endogenous force) are functionally linked through ERK and ROCK and that they cooperate to modulate tissue behavior by regulating FA formation and GF signaling. Matrix stiffness influences tissue growth and morphogenesis by modulating cell contractility, and tensional homeostasis appears to be necessary for normal tissue behavior. These findings provide a fresh perspective for appreciating the role of the tissue microenvironment in differentiation and tumorigenesis, and for identifying tumor therapies.

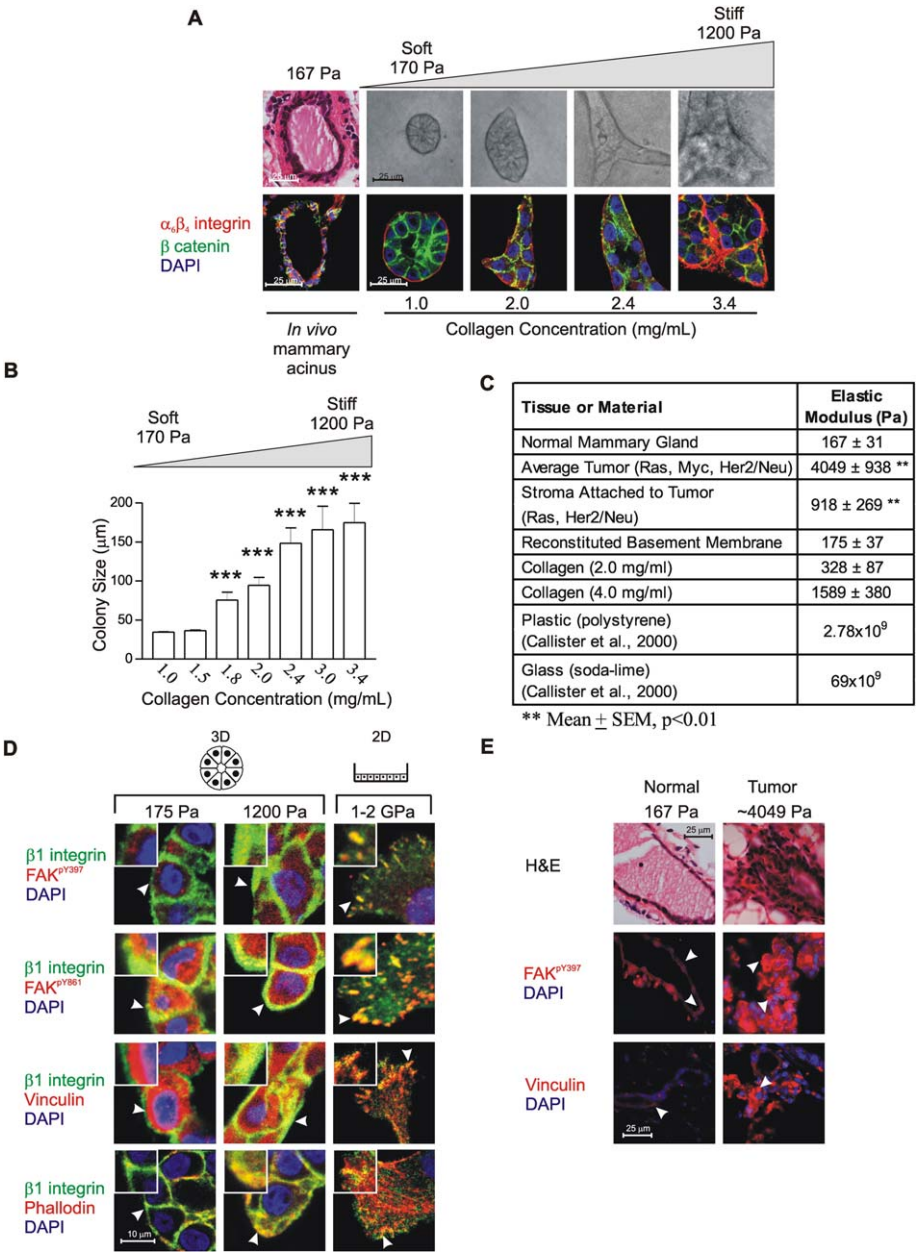

Figure 1. Matrix rigidity regulates growth, morphogenesis, and integrin adhesions

A: Top right: phase images and H&E-stained tissue showing typical morphology of a mammary gland duct in a compliant gland (167 Pa), compared with MEC colonies grown in BM/COL I gels of increasing stiffness (170–1200 Pa). Bottom: confocal immunofluorescence (IF) images of tissue section of a mammary duct and cryosections of MEC colonies grown as above, stained for β-catenin (green), α6 or β4 integrin (red), and nuclei (blue).

B: Colony size of MECs grown as described in **A**. ***$p \leq 0.001$.

C: Elastic modulus of normal mouse mammary gland and established tumors from MMTV-*Her2/neu*, *Myc*, and *Ras* transgenic mice; average value for tumor-adjacent stroma, compared with BM and COL gels; and typical glass and polystyrene substrates used for monolayer culture. Values represent the mean ± SEM of four measurements from multiple mice and gels. **$p \leq 0.01$.

D: Confocal IF images of β1 integrin adhesions (green) in MECs in BM/COL I gels of 175 and 1200 Pa for 16 days (3D BM; soft versus stiff), or 70% confluent monolayers on BM-coated polystyrene (2D stiff), costained for FAK^{pY397}, FAK^{pY861}, vinculin (red), or actin (red) and nuclei (blue). An enlargement of this panel is included in the Supplemental Data.

E: Confocal IF images of FAK^{pY397}, vinculin (red), and nuclei (blue) in MECs in normal and tumor mouse mammary tissue.

"stiff" tumors (Fritz et al., 1999), and activating ROCK induces tumor dissemination (Croft et al., 2004). Therefore, tissue stiffening could drive transformation by increasing Rho-generated cytoskeletal tension.

Integrins are transmembrane ECM receptors that can function as mechanotransducers (Bershadsky et al., 2003), integrins regulate Rho- and GF-ERK-dependent growth (Lee and Juliano, 2004), and ERK influences ROCK and myosin activity (Huang et al., 2004; Vial et al., 2003). Exogenous force can activate integrins (Tzima et al., 2001), drive adhesion assembly (Galbraith et al., 2002), and influence FA formation (Riveline et al., 2001). Moreover, Rho-generated cytoskeletal tension promotes FA assembly and drives ERK-dependent growth (Chrzanowska-Wodnicka and Burridge, 1996), and cytoskeletal reinforcement of integrins is required for FAK^{pY397} phosphorylation (Shi and Boettiger, 2003). Furthermore, integrin expression is higher in epithelia on rigid two-dimensional (2D) substrata than on a compliant 3D matrix (Delcommenne and Streuli, 1995), and matrix rigidity increases integrin expression (Yeung et al., 2005). Thus, tissue stiffness could drive expression of a malignant phenotype through force-dependent regulation of integrin expression, activity, or adhesions. Indeed, integrin levels and signaling are altered in "stiff" tumors (Guo and Giancotti, 2004), and integrins and Rho GTPases can modify the tumorigenic behavior of a tissue (Liu et al., 2004; White et al., 2004). Here, we asked if and how tissue stiffening could drive malignant behavior of a tissue through Rho-dependent integrin modulation.

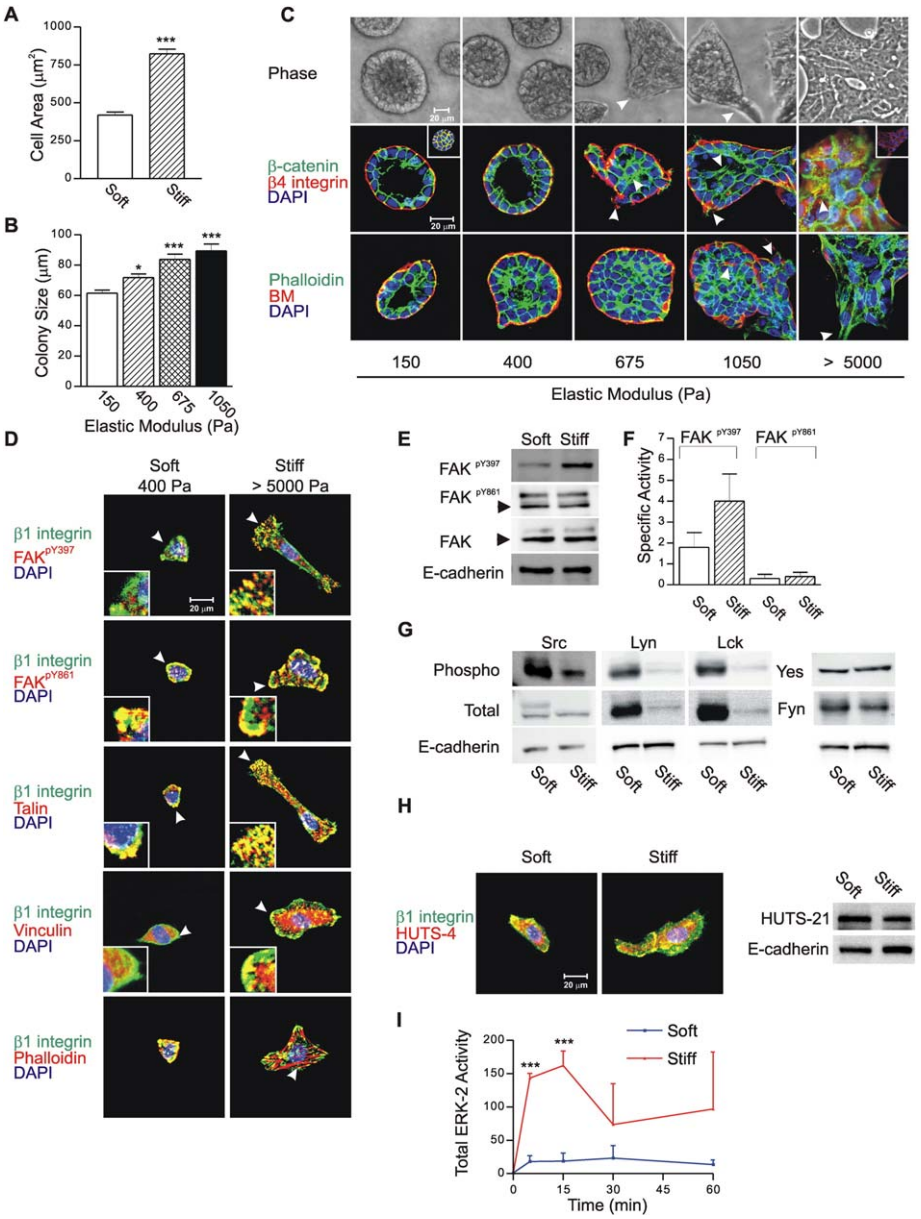

Figure 2. Matrix stiffness modulates integrin adhesions to regulate MEC growth and behavior

A: Cell area for MECs on soft and stiff BM-cross-linked PA gels.

B: Colony size of MEC spheroids on BM gels of increasing stiffness (150–5000 Pa), overlaid with BM to induce morphogenesis (3D BM gel).

C: Phase contrast microscopy and confocal IF images of MEC colonies on 3D BM gels of increasing stiffness (150–5000 Pa), showing colony morphology after 20 days (top); β-catenin before (large image) and after triton extraction (inset; see also Supplemental Data) (green), costained with β4 integrin (large image) or E-cadherin (inset) (red; middle); and actin (green), costained with LN-5 (BM; red; bottom) and nuclei (blue).

D: Confocal IF images of β1 integrin adhesions (green) in MECs on soft and stiff BM gels (400 versus 5000 Pa), costained for FAK^{pY397}, FAK^{pY861}, talin, vinculin (red), actin (red), and nuclei (blue). Inset: 3× magnification. An enlargement of this panel is included in the Supplemental Data.

E: Representative immunoblot of total and phospho-FAK and E-cadherin in MECs on soft and stiff BM gels.

F: Quantification of E-cadherin-normalized FAK immunoblot results shown in **E**.

G: Immunoblot analysis of Src family kinases and E-cadherin in MECs on soft and stiff BM gels.

H: Left: confocal IF images of activated β1 integrin (red; HUTS-4), costained with total β1 integrin (green) and nuclei (blue). Right: representative immunoblot of ligand bound β1 integrin (HUTS-21 binding) in MECs on soft and stiff BM gels.

I: Graph showing immunoblot quantification of EGF-induced (20 ng/ml) phospho-ERK normalized to E-cadherin in MECs on soft and stiff BM gels for 4 days.

A and **B** represent ≈400 measurements from three experiments. **A**, **B**, **F**, and **I** are mean ± SEM of three experiments. Cells in **A**, **D**, **E**, **G**, and **H** were on gels for 24 hr. *$p \leq 0.05$; ***$p \leq 0.001$.

Results

Matrix rigidity regulates growth, morphogenesis, and integrin adhesions

The mammary gland develops within a fat pad and represents one of the more compliant tissues in the body (Figure 1A). We reasoned that mammary differentiation and tissue homeostasis would be most favored by a soft tissue microenvironment and that breast desmoplasia and tissue stiffening that accompany mammary tumor development might therefore actively promote malignant behavior of the gland (Azar et al., 2001). To test this possibility, an electro-mechanical indentor was used to conduct unconfined compression analysis of normal and malignant breast tissues from MMTV-*Her2/neu*, *Myc*, and *Ras* transgenic mice. Normal mammary tissue was found to be extremely soft, whereas the stromal matrix adjacent to the transformed cells and the tumor itself was quite stiff (Figure 1C). Reconstituted ECMs, such as 1 mg/ml collagen (COL) gels and basement membrane (BM) gels, that support normal mammary tissue morphogenesis in culture were also very soft, with elastic moduli virtually identical to normal mammary tissue. COL gels used to study branching morphogenesis had an intermediate stiffness, and gels and substrata that do not support normal tissue morphogenesis such as polystyrene (tissue culture plastic) and soda lime glass were exceedingly rigid (Callister, 2000).

To explore the role of matrix stiffness in mammary tissue behavior, BM/COL I gels were produced with constant BM (to permit laminin [LN]-dependent acini morphogenesis), and the COL levels were varied to recapitulate the range of stiffness between normal mammary gland and tumors. When BM/COL compliance was matched to that of a normal mammary stroma (compare 167 to 170 Pa), nonmalignant MCF10A (Figures 1A

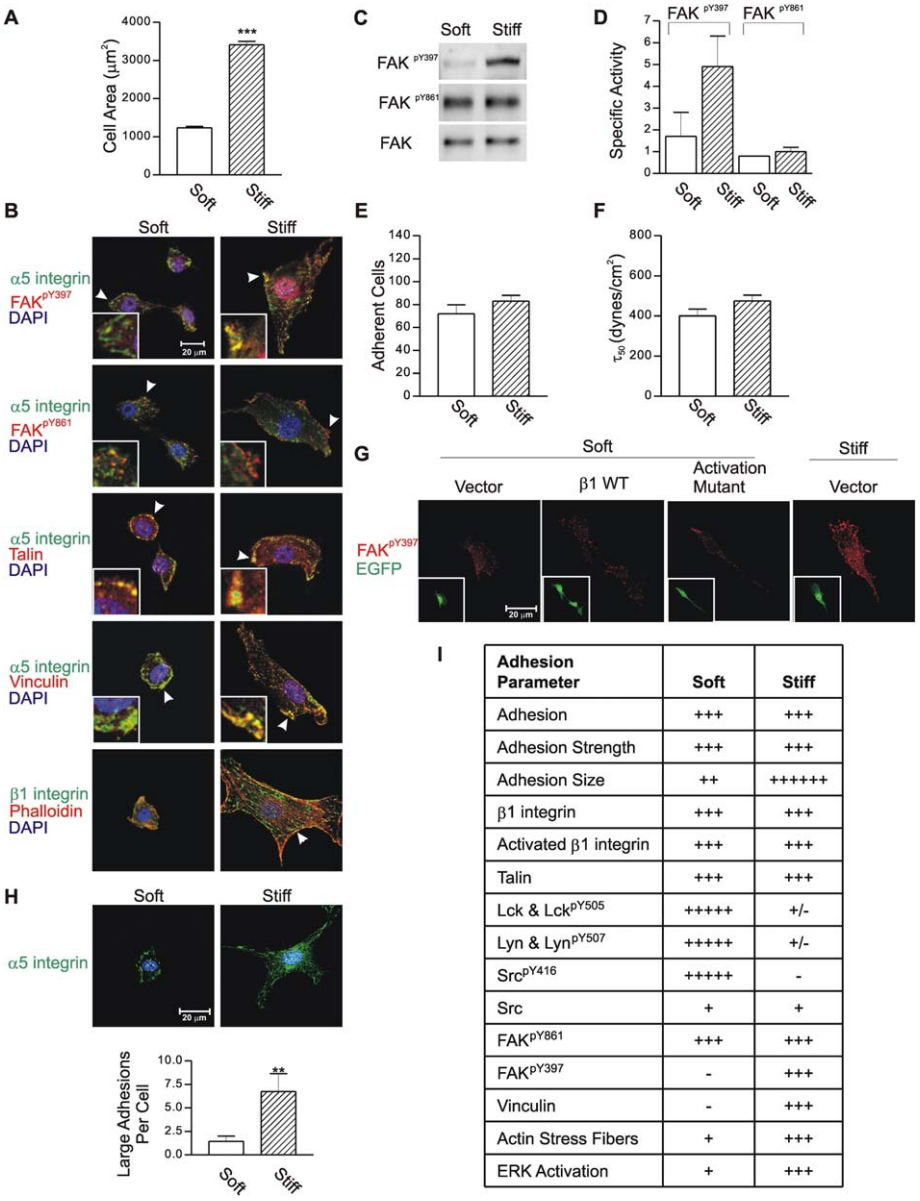

I

Adhesion Parameter	Soft	Stiff
Adhesion	+++	+++
Adhesion Strength	+++	+++
Adhesion Size	++	++++++
β1 integrin	+++	+++
Activated β1 integrin	+++	+++
Talin	+++	+++
Lck & Lck^{pY505}	+++++	+/-
Lyn & Lyn^{pY507}	+++++	+/-
Src^{pY416}	+++++	-
Src	+	+
FAK^{pY861}	+++	+++
FAK^{pY397}	-	+++
Vinculin	-	+++
Actin Stress Fibers	+	+++
ERK Activation	+	+++

Figure 3. Matrix rigidity regulates cell behavior by inducing FAs

A: Cell spreading quantified as cell area for fibroblasts on soft and stiff FN gels. Values represent ≈400 measurements from three experiments. ***$p \leq 0.001$.

B: Confocal IF images of α5(β1) integrin adhesions (green) in fibroblasts on soft and stiff FN gels (400 versus 5000 Pa) costained for FAK^{pY397}, FAK^{pY861}, talin, vinculin (red), actin (red), and nuclei (blue). An enlargement of this panel is included in the Supplemental Data.

C: Representative immunoblot of total and phospho-FAK protein in fibroblasts on soft and stiff FN gels.

D: Quantification of immunoblot results shown in **C**.

E: Relative fibroblast adhesion on soft and stiff FN gels.

F: Quantification of shear force required to detach fibroblasts from soft (1050 Pa) and stiff (66 kPa) FN gels.

G: Confocal IF images of FAK^{pY397} (red), EGFP (inset; green), and nuclei (blue) in fibroblasts expressing exogenous EGFP vector (Vector), wild-type β1 integrin, and EGFP vector (β1 WT), or a constitutively activated β1 glycan wedge G429N integrin and EGFP vector (Activation Mutant) on a soft FN gel, compared to fibroblasts expressing EGFP vector (Vector) on a stiff FN gel.

H: Confocal IF images of α5(β1) integrin (EGFP; green) in fibroblasts on soft and stiff FN gels. **$p \leq 0.01$.

I: Summary of experimental results from Figures 1–3. Regardless of cell or matrix type, cells interacting with a soft matrix assemble focal complexes and express high amounts of total and active Src family kinase, whereas on a stiff matrix cells spread and assemble stress fibers, activate more ERK in response to growth factors, and form FAs with FAK^{pY397} and vinculin.

Experiments reported for **D**–**F** and **H** are mean ± SEM of three experiments.

and 1B) and HMT3522 S-1 MECs (data not shown) formed small growth-arrested and polarized acini with AJs and a central lumen (compare tissue acinus to acini formed in a 1 mg/ml floating BM/COL gel). Yet, even a small increase in matrix stiffness (170–1200 Pa) significantly increased EGF-dependent growth (Figure 1B), compromised tissue organization, inhibited lumen formation, and destabilized AJs (indicated by diffuse β-catenin [Figure 1A] and triton-extractable and noncolocalized β-catenin and E-cadherin [data not shown]). Interestingly, disruption of basal polarity, visualized by diffuse β4 integrin localization, required a substantial increase in matrix rigidity (compare 170 to 1200 Pa; Figure 1A).

Because integrins are mechanotransducers that relay ECM cues, the effect of matrix stiffness on integrin function was analyzed by assessing colocalization of components involved in mechanosignaling with (α3)β1 integrin. MECs interacting in 3D with a soft (175 Pa) and stiff (1200 Pa) BM, and in 2D with a stiff BM (1–2 GPa), formed (α3)β1 integrin adhesions, indicated by FAK^{pY861} (Figure 1D) and talin (data not shown) that colocalized with β1 integrin. However, MECs could only phosphorylate FAK^{pY397} and recruit vinculin to their (α3)β1 integrin adhesions when interacting in 2D or 3D with a rigid BM (Figure 1D). These data indicate that a stiff matrix, whether in 2D or 3D, is incompatible with normal tissue morphogenesis and that matrix stiffness may modulate integrin adhesions. Because a similar correlation between tissue stiffness and FAK^{pY397} and vinculin expression in normal and malignant tissues in vivo was also observed (Figure 1E), this suggests that tissue stiffness could contribute to aberrant epithelial tissue behavior by influencing integrin adhesions.

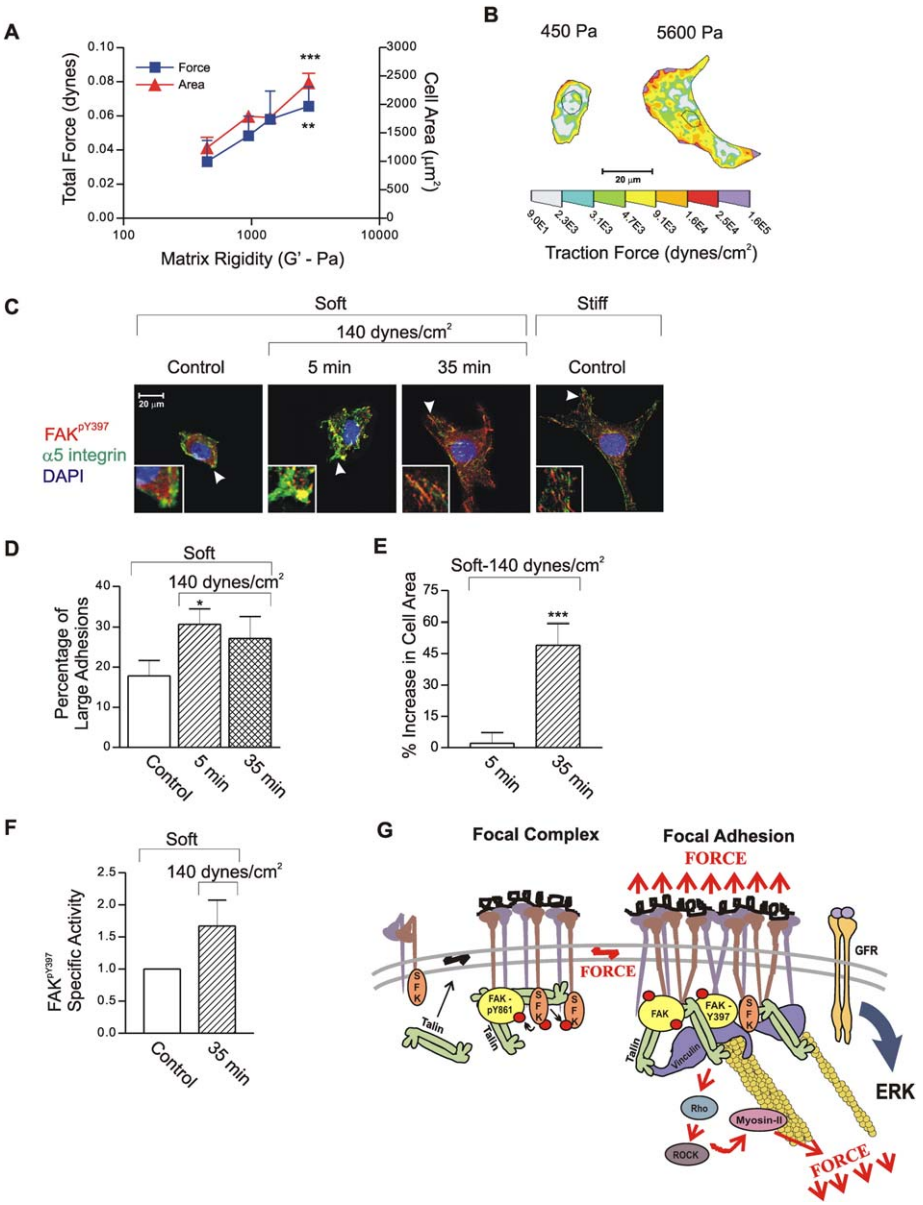

Figure 4. Force-dependent integrin aggregation, FAs, and cell behavior

A: Correlation between matrix rigidity, fibroblast area, and fibroblast contractility (quantified by TFM).

B: Representative traction map showing typical force distribution in fibroblasts on soft (450 Pa) and stiff FN gels (5600 Pa).

C: Confocal IF images showing time course of changes in α5β1 integrin (green), FAK^{pY397} (red), and nuclei (blue) in fibroblasts on soft FN gels before (Soft; Control) and after (Soft; 5 and 35 min) 140 dynes shear force. An enlargement of this panel is included in the Supplemental Data.

D: Adhesion size in fibroblasts on soft FN gels before (Control) and after (5 min) shear force, and additional incubation.

E: Graph showing no change in fibroblast spreading 5 min after 140 dynes shear force, but a significant increase after 30 min incubation (35 min).

F: Bar graph showing increased FAK^{pY397} relative to total FAK in fibroblasts on soft FN gels after 140 dynes shear stress (5 min) and 30 min incubation (35 min).

G: Model of force-dependent FA assembly.

Matrix stiffness modulates integrin adhesions to regulate MEC growth and behavior

COL gels are inherently variable, and elevating matrix stiffness by increasing COL concentration could confound data interpretation through altered integrin occupancy. To address this, we used BM-crosslinked polyacrylamide (PA) gels (BM gel) with calibrated elastic moduli of 150, 400, 675, 1050, and ≥5000 Pa. Similar to MECs inside a 3D BM (3D BM; Weaver et al., 2002) or on top of a thick BM overlaid with BM (3D over BM; Debnath et al., 2003), by 16–20 days MECs on a compliant PA BM gel overlaid with BM (3D BM gel) formed growth-arrested acini with cell-cell localized β-catenin, basally polarized β4 integrin, and apical-lateral cortical actin and assembled an endogenous LN-5 BM (Figure 2C). Similar to results with 3D COL gels, increasing matrix rigidity (from 150 to 400 to 675 to 1050) progressively increased EGF-dependent ERK activation and colony size (Figures 2B and 2I), hindered lumen formation, destabilized AJs, and perturbed tissue polarity (absence of β-catenin/E-cadherin colocalization and triton-extractable β-catenin [Figure 2C and inset], disrupted localization of β4 integrin and LN-5, and progressive filling of the spheroid lumens; Figure 2C). Intriguingly, actin stress fibers were not observed in any of these cultures until matrix rigidity increased to 5000 Pa, toward that measured in tumors (≈4049 Pa) and in MECs on highly rigid 2D substrata (1–2 GPa; Figures 1 and 2D, phalloidin).

Because MEC colonies initiate clonally, the effect of matrix compliance on MEC behavior and integrin adhesions in isolated cells was examined. Within 12 hr of plating, MECs spread significantly more on stiff versus soft BM gels (Figure 2A). Yet, MECs adhered rapidly, activated β1 integrin (Figure 2H), and recruited talin and FAK^{pY861} to β1 integrin adhesions (Figures 2D–2F) equally on soft and stiff BM gels, indicating that MECs

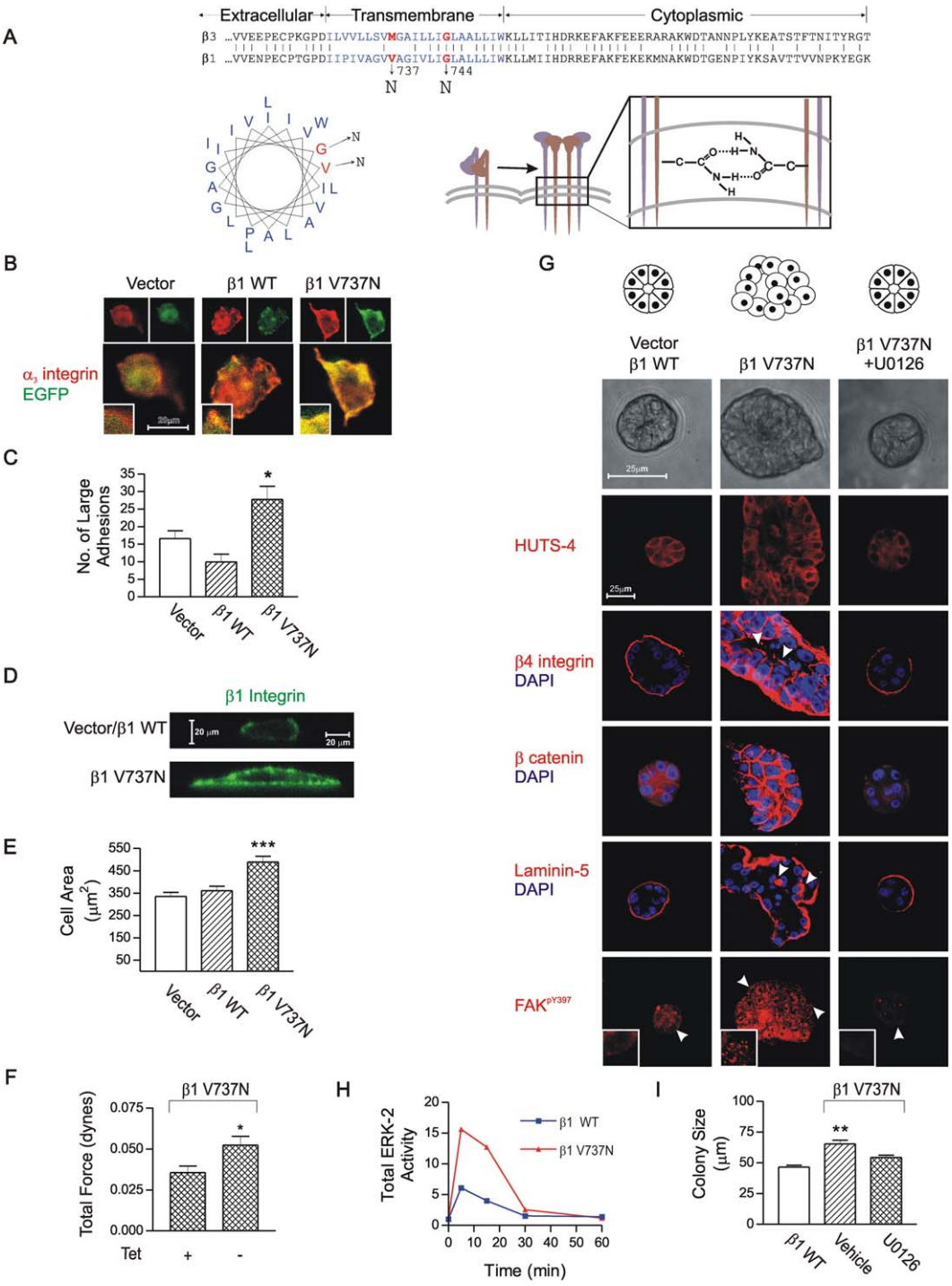

Figure 5. Integrin clustering enhances ERK activation and cell contractility to perturb tissue behavior

A: Bottom right: alignment of the C-terminal 82 amino acids of the human β3 and β1 integrin with incorporated amino acid substitutions indicated. Bottom left: a helical wheel representing the β1 integrin transmembrane domain indicating that V737 and G744 lie on the same face of the helix separated by two turns.

B: Confocal IF images of α3 integrin (red; top left), EGFP-tagged wild-type, and mutant β1 integrin (EGFP; green; top right), with α3 and β1 integrin overlay (yellow; bottom).

C: Adhesion size in MECs expressing the EGFP vector (Vector), EGFP-tagged wild-type (β1 WT), and V737N β1 integrin (β1 V737N).

D: Confocal IF vertical image showing aggregates of β1 integrin in MECs expressing the V737N mutant (green), compared to MECs expressing wild-type β1 integrin.

E: Cell area of MECs on soft BM gels expressing EGFP vector (Vector), EGFP-tagged wild-type β1 integrin (β1 WT), or V737N β1 integrin (β1 V737N).

F: Bar graph of force exerted by cells on soft gels expressing V737N β1 integrin (Tet−; β1 V737N) compared to tetracycline-treated controls (Tet+; control).

could assemble integrin adhesions under both conditions. Indeed, MECs on soft BM gels had higher levels of total and activated Lyn^{pY507} and Lck^{pY505} kinases than MECs on stiff gels (Figure 2G), and MECs grew and survived in 3D quite well, consistent with integrin activation, FAK^{pY861}, and adhesion assembly (Arias-Salgado et al., 2003). Because cells suspended in the absence of ECM also lacked FAK^{pY861} and FAK^{pY397}, but could phosphorylate FAK^{pY861} upon antibody-induced or polymerized ligand-mediated integrin clustering (Supplemental Data; Shi and Boettiger, 2003), this suggests that MECs on soft BM gels likely assemble focal complexes as opposed to FAs. Indeed, only MECs interacting with a stiff BM gel, or a stiff tissue stroma, could phosphorylate FAK^{pY397} and recruit vinculin to (α3)β1 integrin adhesions (Figures 1D, 1E, and 2D–2F), suggesting that matrix stiffness is necessary for FA assembly or stabilization. Consistently, MECs on stiff gels activated and sustained more ERK and grew better in response to EGF (Figure 2I), comparable to fibroblasts on a rigid fibronectin (FN) substrate that sustain ERK activity only when FAs are present (Roovers and Assoian, 2003).

Matrix rigidity regulates cell behavior by inducing FAs

To understand how ECM rigidity could regulate integrin adhesions, the effect of matrix compliance on α5β1 integrin-FN adhesions and fibroblast behavior was also assessed. Identical to MECs on BM gels, fibroblasts on soft and stiff FN-cross-linked PA gels (FN gel) adhered and recruited talin and FAK^{pY861} comparably at α5β1 integrin adhesions (Figure 3B). Moreover, only fibroblasts interacting with a stiff FN gel assembled actin stress fibers, phosphorylated FAK^{pY397}, and recruited vinculin to α5β1 integrin adhesions (Figures 3B–3D). Fibroblasts also spread significantly better on stiff versus soft FN gels (Figure 3A). Interestingly, fibroblasts adhered equally to soft and stiff FN gels (Figure 3E), and when adhesion strength was measured using a spinning disc apparatus (Shi and Boettiger, 2003) fibroblasts detached with virtually the same force per cm^2 from soft and stiff FN gels (Figure 3F), suggesting that they adhere with the same strength regardless of matrix compliance. Consistently, ectopic expression of neither wild-type α5 integrin (Yeung et al., 2005), nor wild-type β1 integrin (Figure 3G), nor even a constitutively active G429N β1 integrin glycan wedge mutant (Luo et al., 2004) could increase FAK^{pY397} or drive fibroblast spreading on a soft FN gel. Instead, α5β1 integrin adhesions were much larger in fibroblasts spread on stiff FN gels (Figure 3H), implying that cells on compliant gels form focal complexes and that a stiff matrix alters cell behavior by promoting FAs (Figure 3I).

Force-dependent integrin aggregation, FAs, and cell behavior

FAK^{pY397} and vinculin recruitment to integrin adhesions requires force (Galbraith et al., 2002; Shi and Boettiger, 2003), matrix stiffness modulates cell contractility (Wang et al., 2000), and Rho-induced cytoskeletal tension clusters integrins (Chrzanowska-Wodnicka and Burridge, 1996). Consistently, traction force microscopy (TFM) showed that contractility (integral of the force magnitudes), cell spreading (cell area), and FAK^{pY397} (data not shown) positively correlate with matrix rigidity (Figures 4A and 4B), confirming that force is likely required for FA assembly and/or stabilization. To directly test this prediction, fibroblasts on soft FN gels were subjected to an exogenous shear force, and a correlation between force magnitude and the timing of the appearance of FAs and cell spreading was assessed. A 5 min shear force of 100–140 dynes was sufficient to increase the size of α5β1 integrin adhesions and induce FAK^{pY397} and cell spreading (Figures 4C–4F). Yet, integrin clustering preceded rather than followed the appearance of FAK^{pY397} and cell spreading (lag time 20–30 min; Figures 4C–4F), implying that force-dependent integrin aggregation (anisotropy) promotes FA assembly (Nicolas et al., 2004).

Integrin clustering enhances ERK activation and induces cell tension to perturb tissue behavior

Because force-dependent integrin aggregation preceded FA assembly, β1 integrin mutants with increased transmembrane molecular associations were generated to test whether integrin anisotropy could drive FA formation. Hydrophobic valine 737 was replaced with hydrophilic asparagine (V737N), or neutral glycine 744 was replaced with asparagine (G744N), to promote integrin self-association through enhanced hydrogen bonding in the transmembrane domain (Li et al., 2003), and cells expressing the mutant integrins were assayed for their behavior on compliant gels. Untagged (data not shown) and EGFP-tagged wild-type and mutant V737N (Figure 5B) and G744N (data not shown) β1 integrin expressed equally well in MECs and fibroblasts (data not shown), colocalized with integrins at sites of matrix adhesion (Figure 5B), adhered similarly (data not shown), and had comparable levels of cell surface β1 and β4 integrin (data not shown) and ligand bound integrin (Supplemental Data). Enhancing integrin associations did not induce integrin clustering when cells were plated on a rigid matrix (e.g., tissue culture plastic; Luo et al., 2005); however, on soft gels (analogous to cells in suspension with no tension; Li et al., 2003), V737N β1 integrin-expressing cells spread significantly more (Figures 5D and 5E), formed larger integrin adhesions (Figures 5C and 5D) with more FAK^{pY397} (Figure 5G), and activated more ERK in response to GF stimulation (Figure 5H). V737N β1 integrin-expressing cells exerted greater force (Figure 5F), and V737N β1 integrin-expressing MECs exhibited aberrant morphogenetic behavior, in response to a compliant matrix (V737N β1 integrin MECs formed larger, nonpolarized colonies lacking AJs and assembled spheroids lacking a completely cleared lumens; Figures 5G and 5I), but the abnormal

G: Phase contrast and confocal images of activated β1 integrin (HUTS-4), β4 integrin, β-catenin, LN-5, and FAK^{pY397} (red) in MEC colonies expressing EGFP-tagged wild-type β1 integrin (β1 WT), compared to the EGFP-tagged V737N β1 integrin (β1V737N), with and without the MEK inhibitor U0126, after 16 days in BM. Inset: 2× magnification.

H: Quantification of immunoblot results of EGF-dependent (20 ng/ml) phospho-ERK activity normalized to E-cadherin in wild-type β1 integrin and β1V737N-expressing MECs on soft BM gels for 24 hr.

I: Colony size of MECs expressing the EGFP-tagged wild-type β1 integrin (β1 WT) or V737N β1 integrin (β1 V737N) treated with or without U0126 for 16 days in BM.

C, **E**, **F**, and **H** are mean ± SEM of three experiments, and **E**, **F**, and **H** consist of ≈400 measurements. *$p \leq 0.05$; **$p \leq 0.01$; ***$p \leq 0.001$.

phenotype could be phenotypically reverted if ERK activity was repressed (Figures 5G and 5I). These data extend previous work highlighting the existence of a functional link between cytoskeletal tension-regulated FA assembly and ERK-dependent growth to show that matrix compliance (exogenous force) can influence tissue phenotype by regulating integrin aggregation to enhance GF-dependent ERK activation, induce cell tension (endogenous force), and drive or stabilize FA assembly.

Matrix stiffness induces integrin clustering to enhance GF-dependent ERK activation and Rho-generated force, thereby modifying tissue growth and morphology

Integrins regulate Rho GTPases, cells employ myosins for contractility, and myosin activity is regulated by Rho (Burridge and Wennerberg, 2004). We found that matrix rigidity increases Rho activity (Figure 6B), and inhibiting ROCK using Y-27632, or myosins using ML-7 or Blebbistatin (data not shown), significantly reduces cell-generated force (Figure 6A). Moreover, expressing a constitutively active V14Rho elevates cell-generated force (Figure 6C), increases the number and size of FAs (Figure 6E), and significantly increases cell spreading on a soft gel (Figures 6D and 6E). V14Rho also increases the size of EGF-dependent mammary colonies in BM (Figure 6G), increases FAs (see vinculin and FAK^{pY397}; Figure 6F), and compromises MEC morphogenesis (diffuse β-catenin and absence of cleared lumens; Figure 6F). Nevertheless, the aberrant V14Rho tissue phenotype could be phenotypically normalized by inhibiting EGF-dependent ERK activation (using the U0126 MEK inhibitor) or by inhibiting cell contractility (using a myosin II inhibitor, Blebbistatin), and ERK inhibition decreased cytoskeletal tension (endogenous force) and reduced ROCK levels (Figures 6H and 6I; see also Supplemental Data). This indicates that matrix compliance (exogenous force)-dependent integrin clustering regulates GF-dependent ERK activation to control cell growth and tissue behavior by influencing Rho-generated cytoskeletal tension and FA formation.

GF signaling, Rho-dependent tension, FAs, and the malignant phenotype

Similar to primary normal and malignant MECs, nonmalignant EGF-dependent S-1 MECs from the HMT3522 tumor progression series assemble acini in BM, whereas their EGFR-transformed T4-2 progeny form continuously growing, disorganized, and invasive colonies (Figure 7F, compare S-1 to T4-2). Yet, these T4-2s, which form abundant FAs (Figure 7B) and have elevated EGF-dependent ERK activity, can be phenotypically reverted to form polarized and growth-arrested acini if β1 integrin, EGFR, or ERK activity is inhibited (Wang et al., 1998). Consistent with a model in which an ECM compliance (exogenous force)-integrin-GF-ERK-Rho signaling circuit links cytoskeletal tension to cell growth and tissue phenotype, T4-2s spread more (Figure 7E) and exert significantly higher force on a soft BM gel, as compared to S-1s (Figures 7C and 7D). T4-2s also have higher Rho activity (Figure 7A), and inhibiting Rho or myosin activity by expressing a dominant-negative N19Rho (Figure 7B; green inset), or by treatment with Y-27632 or Blebbistatin, significantly represses T4-2 contractility and cell spreading (compare T4-2s to N19Rho, Y-27632, and Blebbistatin T4-2s; Figures 7B–7D). Reducing Rho-ROCK-dependent cytoskeletal tension in these mammary tumors also reduces FAK^{pY397}, reestablishes tissue polarity (basal β4 integrin and LN-5), restores cell-cell interactions (less diffuse β-catenin), permits lumen formation, and reduces colony size (Figures 7B, 7F, and 7G). Normalizing tumor cytoskeletal tension also reduces ROCK expression and ERK activity (Figure 7J) and lowers total and activated EGFR (Figure 7I), which could explain the significant reduction in proliferation and cytoskeletal tension also observed (Figures 7C, 7D, and 7H). Thus, although in tumors integrin and GF-dependent ERK activation can become uncoupled from exogenous force cues (matrix stiffness), some transformed cells do retain functional links between cytoskeletal tension and Rho signaling, such that normalizing mechanosignaling can repress their malignant phenotype.

Discussion

Tissue stiffness can predict the presence of a tumor or the development of pathology with a heightened risk of malignant transformation, yet the relevance of tissue rigidity to tumor pathogenesis has been largely ignored. We showed that tumor rigidity reflects an increase in stromal stiffness and tumor cell tension. We found that even a small increase in matrix rigidity will perturb tissue architecture and enhance growth by inducing Rho-generated cytoskeletal tension to promote FA assembly and increase GF-dependent ERK activation. We determined that a highly contractile, EGFR-transformed epithelium with elevated Rho and ERK activity can be phenotypically reverted to form differentiated acini lacking FAs with reduced EGFR activity if Rho-generated cytoskeletal tension or ERK activity is decreased. Accordingly, these data underscore the potential existence of a mechanoregulatory circuit that functions to integrate physical cues from the ECM (exogenous force) with FA assembly through ERK- and Rho-dependent cytoskeletal contractility to regulate cell and tissue phenotype (Figure 8). Thus, tensional homeostasis may be essential for normal tissue growth and differentiation, and increasing tissue rigidity by stiffening the matrix (fibrosis) or by elevating Rho signaling through, for example, oncogene (*Ras*)-driven ERK activation, could induce cytoskeletal contractility to enhance integrin-dependent growth and destabilize tissue architecture (Zhong et al., 1997). As such, conditions that induce tissue fibrosis (matrix stiffening; Akiri et al., 2003) or situations that amplify oncogene activity to enhance ERK could facilitate malignant transformation by increasing cell contractility through Rho. Because we found that transformed cells can retain a functional link between Rho-dependent cytoskeletal tension, integrins, and growth regulation, pharmacological inhibitors that target ROCK, ERK, or integrin adhesions could temper the malignant behavior of some tumors by normalizing activity through the cellular mechanocircuitry.

Pertinent to the study of cancer biology is an understanding of how normal tissue differentiation is achieved. Three-dimensional ECM culture models have highlighted the importance of matrix compliance for tissue-specific differentiation and imply that cells in 3D might respond differently to growth, polarity, and death stimuli (O'Brien et al., 2002; Paszek and Weaver, 2004; Wang et al., 1998; Weaver et al., 2002). We found that matrix compliance differs dramatically between 2D and 3D cultures, and normal versus tumor tissue in vivo, and that faithful recapitulation of normal tissue morphogenesis is favored by matrix conditions with an elastic modulus that corresponds with normal tissues in vivo. Our observations are consistent

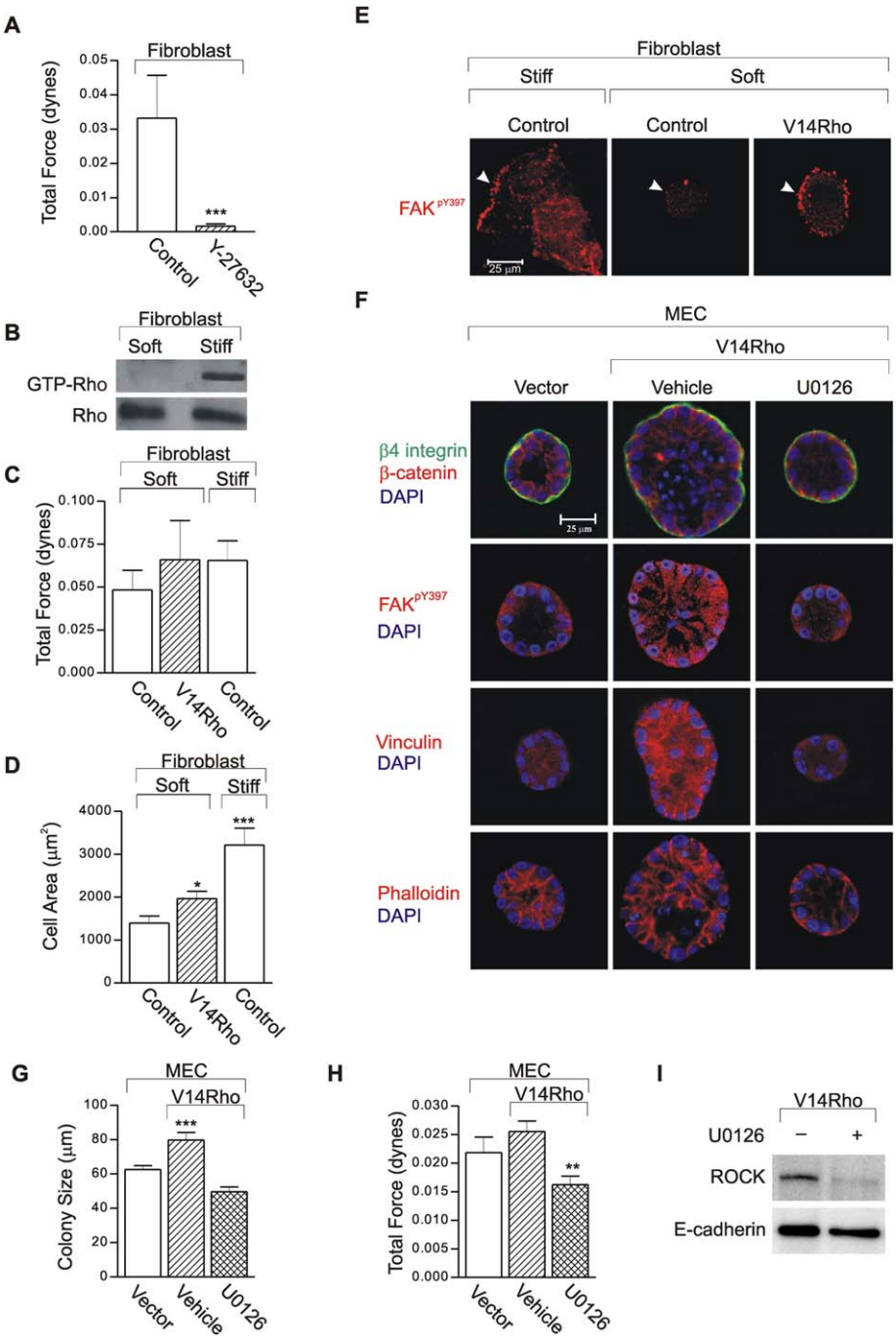

Figure 6. Matrix stiffness induces integrin clustering to enhance GF-dependent ERK activation and Rho-generated tension, increase growth, and perturb tissue morphology

A: Cell force quantified by TFM in fibroblasts on a FN gel, treated with vehicle or the ROCK inhibitor Y-27632.

B: Representative immunoblot and quantification of immunoprecipitated Rhotekin-associated Rho (GTP-Rho) and total Rho (Rho), in fibroblasts on soft and stiff FN gels.

C: Cell force using TFM of vector control (Control) and V14Rho-expressing fibroblasts on soft (450 Pa) and stiff (5600 Pa) FN gels.

D: Cell area of vector control (Control) and V14Rho-expressing fibroblasts on soft and stiff FN gels.

E: Confocal IF images of FAK^{pY397} (red) in control or V14Rho-expressing fibroblasts.

F: Confocal IF images of β4 integrin (green), co-stained with β-catenin (red), FAK^{pY397}, vinculin (red), actin (red), and nuclei (blue), in MEC colonies in a compliant (175 Pa) BM for 16 days, expressing either a vector (Vector) or active Rho (V14Rho) treated with vehicle or the MEK-1 inhibitor U0126.

G: Colony size of MECs expressing vector (Vector) or active Rho (V14Rho) treated with vehicle or U0126, in BM for 16 days.

H: Total force (TFM) exerted by V14Rho MECs on soft gels treated with vehicle or U0126.

I: Representative immunoblot of ROCK expressed in V14Rho MECs treated with vehicle or U0126.

Results in **G** are mean ± SEM of three experiments; **A**, **C**, and **D** represent ≈50 measurements. *p ≤ 0.05; **p ≤ 0.01; ***p ≤ 0.001.

with the role shown for matrix compliance in smooth muscle cell differentiation (Engler et al., 2004) and extend those findings to incorporate the effect of matrix stiffness on multicellular epithelial tissue morphogenesis. We also identified a plausible mechanism for these effects by showing how matrix compliance can influence cell fate by regulating Rho-generated cytoskeletal tension to induce FA assembly and enhance integrin-dependent GF-induced activation of ERK. Moreover, we determined that some transformed cells have altered tensional homeostasis, which could partly explain why some malignant cells can grow and survive in the absence of exogenous matrix tension (i.e., in suspension), fail to undergo differentiation in compliant 3D ECMs, and have elevated FAK^{pY397} in culture and in vivo (Lark et al., 2005; McLean et al., 2004; Wang et al., 2000; Wozniak et al., 2003). By illustrating how exogenous force and cytoskeletal tension are integrated, and how they could cooperate to influence integrin adhesions and GF-dependent activation of ERK, our studies offer a fresh perspective for understanding the molecular basis of tissue differentiation and tumor formation.

Adherent cells interrogate the physical properties of their

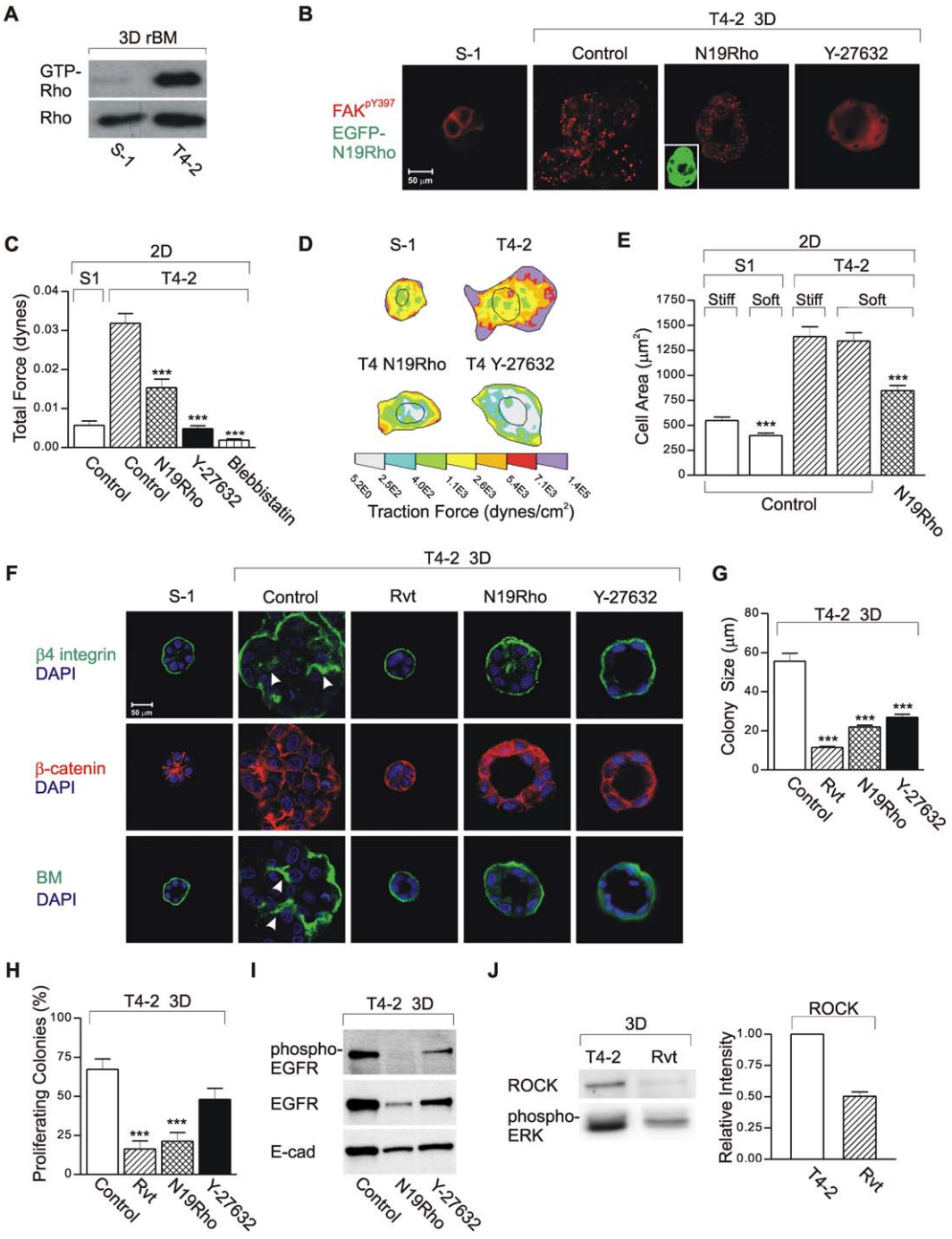

Figure 7. Growth factor signaling, Rho-generated contractility, FAs, and the malignant phenotype

A: Representative immunoblot of immunoprecipitated Rhotekin-associated Rho (GTP-Rho) and total Rho (Rho), in S-1 nonmalignant (S-1) and T4-2 malignant (T4-2) MECs.

B: Confocal IF images of FAK^{pY397} (red) in 3D BM colonies of S-1 and T4-2 control (Control), and T4-2s expressing EGFP-tagged N19Rho (EGFP N19Rho; green) or treated with the ROCK inhibitor (Y-27632).

C: Total force (TFM) on soft BM gels exerted by S-1 and control and N19Rho-expressing T4-2s, or T4-2s treated with Y-27632 or Blebbistatin.

D: Representative traction force maps of various MECs on soft BM gels.

E: Cell spreading quantified as cell area in S-1, and T4-2 control and N19Rho T4-2s on soft and stiff BM gels.

F: Confocal IF images of β4 integrin (green), β-catenin (red), and LN-5 (green), costained for nuclei (blue), in S-1 and control, MEK inhibitor-reverted (Rvt), N19Rho-expressing, and Y-27632-treated T4-2 colonies.

G: Colony size of control (Control), MEK inhibitor-reverted (Rvt), N19Rho-expressing (N19Rho), and ROCK-inhibited (Y-27632) T4-2 MECs.

H: Cell proliferation measured as percent Ki-67 labeling in control (Control), MEK inhibitor-reverted (Rvt), N19Rho-expressing (N19Rho), and ROCK-inhibited (Y-27632) T4-2 MECs colonies.

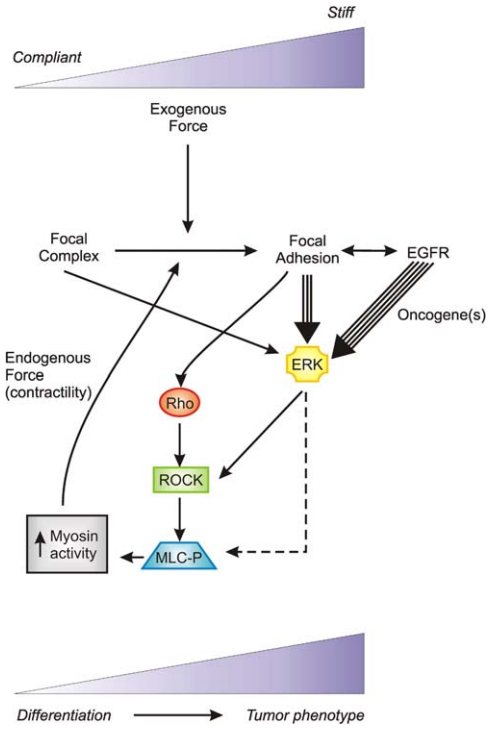

Figure 8. Model of tensional homeostasis and force-dependent malignant transformation

ECM and form integrin adhesions that reflect the compliance of the matrix and the inherent activity of their contractile machinery (Bershadsky et al., 2003). We showed that matrix stiffness drives FA assembly to modify GF signaling and cell phenotype by regulating ERK and Rho activity to modulate cell contractility. Using matrices of defined compliance and an exogenous shear force, we showed that a force threshold exists that favors integrin aggregation and FA assembly. Because we found that integrin clustering precedes and is sufficient for tension-dependent ERK and Rho activity and FA assembly, our data provide compelling evidence in support of the anisotropy adhesion model. This model maintains that the biochemical response of adhesions to cytoskeletal tension originates from the stress-induced elastic deformation of the adhesion site, such that the growth of FAs is mediated by the local density of proteins within the junction via force-initiated interactions (Nicolas et al., 2004).

Malignant transformation is characterized by a reactive stroma, altered stromal-epithelial interactions, and changes in integrins (Guo and Giancotti, 2004; Zahir et al., 2003). Given that integrins facilitate tumor metastasis and can influence expression of the malignant phenotype (Wang et al., 1998; White et al., 2004), it is important to understand how integrins become altered to contribute to malignant transformation. We found that oncogene-induced tumors and their adjacent stroma are significantly stiffer than normal tissue and that matrix rigidity clusters integrins to enhance GF-dependent ERK activation and promotes growth and FA assembly through Rho-dependent cytoskeletal tension. Yet, we also determined that the aberrant morphological structures formed by GF-transformed or V14Rho-expressing cells with elevated ERK- and Rho-dependent cytoskeletal tension can be phenotypically normalized by treatment with either a MEK or myosin II inhibitor. Because inhibitor-mediated phenotypic reversion of these aberrant morphologies was associated with reduced cell force generation (cytoskeletal tension) and reduced ROCK expression, this implies that a functional regulatory circuit exists between integrins, ERK, Rho, and cytoskeletal tension to control cell and tissue behavior. By showing that exogenous force and endogenous force cooperate to regulate cell behavior through FA assembly/stabilization, we maintain that the type of integrin adhesion in a tumor may be more significant than the level of integrins expressed (McLean et al., 2004).

Rho activity is frequently elevated in tumors (Fritz et al., 1999), and ROCK can destabilize AJs (Sahai and Marshall, 2002) and promote tumor invasion and angiogenesis in vivo (Croft et al., 2004; Fritz et al., 1999). Furthermore, patients with inflammatory breast cancer who have elevated ROCK activity show high levels of metastasis and have the worst prognosis (Paszek and Weaver, 2004). Despite these data, the current paradigm maintains that Rho is a tumor suppressor because it promotes stable FAs that impede cell migration. According to this model, the invasive phenotype of *Ras*-transformed cells hinges upon their ability to downregulate ROCK and reduce cell contractility to destabilize FAs and permit cell migration (Sahai et al., 2001). Yet, most studies examining the role of Rho in transformation have been conducted on tissue culture plastic (highly stiff), which greatly enhances Rho activity, GF-dependent ERK activation, FA formation, and cytoskeletal tension. Given that balanced Rac and Rho activity is required for optimal cell migration, culture conditions that elevate Rho-dependent tension could distort experimental observations. By using matrix conditions that match the compliance of normal and transformed tissues in vivo, our data indicate that malignant transformation likely precedes along an exogenous and endogenous force continuum. This paradigm implies that tissue homeostasis is favored by a compliant matrix and low integrin-ERK-Rho-cytoskeletal tension, whereas tumorigenic behavior initiates when the matrix becomes chronically stiffer and/or integrin-ERK-Rho activity rises appreciably and remains elevated for protracted periods of time. A highly stiff matrix or exceedingly high integrin-ERK-Rho signaling would theoretically antagonize tumor invasion because it would promote the assem-

I: Representative immunoblot of total and phospho-EGFR compared to E-cadherin in control (Control), N19Rho-expressing (N19Rho), and ROCK-inhibited (Y-27632) T4-2 MEC colonies.

J: Representative immunoblot of total and phospho-ERK and ROCK compared to E-cadherin in control (T4-2) and phenotypically reverted (Rvt) T4-2 MEC colonies.

Results in **G** and **H** are mean ± SEM of three experiments of ≈200 measurements; **C** and **E** represent ≈50 measurements. ***$p \leq 0.001$. Colonies were in BM for 12 days.

bly of multiple stable FAs. This model could explain why MMTV-*Ras* and *Myc* mammary tumors typically form encapsulated and highly rigid tumors that do not readily metastasize, and why early passages of *Ras*-transformed fibroblasts form abundant stress fibers with numerous FAs and fail to migrate on tissue culture plastic, until ROCK levels decrease (Vial et al., 2003).

In conclusion, ERK and Rho appear to be part of an integrated mechanoregulatory circuit that functions to link physical cues from the stromal ECM through integrin adhesions to molecular pathways that control cell growth and tissue phenotype. A chronic increase in cytoskeletal tension, mediated by sustained matrix stiffness (a prolonged injury or chronic inflammatory response), or through elevated ERK activity (oncogene amplification) if of sufficient magnitude and duration, could drive the assembly/stabilization of FAs to enhance growth and perturb tissue organization, thereby promoting malignant transformation of a tissue.

Experimental procedures

Antibodies and reagents

The following antibodies were used: monoclonal (mAb) COL IV, CIV 22 (Dako); LN-5 α3 chain specific, BM165 (gift P. Marinkovich); β1-integrin, TS2/16 (ATCC), AIIB2 and HUTS-4 and 21, β4 integrin, 3E1; α3 integrin, P15B and α5 integrin, NKI-SAM-1 (Chemicon); E-cadherin, 36; Ki-67, 37; and FAK, 77 (BD Transduction); α5 integrin, 5H10-27 (BD PharMingen); talin, 8D4 and vinculin, VIN-11-5 (Sigma); and Src, 327 (Oncogene Res); polyclonals to FAK^{pY397} and FAK^{pY861} (BioSource), activated Src^{pY416} family kinase, lyn, lck, and ERK, activated lyn^{pY507} and lck^{pY505} and ERK (p44/p42; Cell Signaling); fyn and yes (Santa Cruz Biotech); β-catenin (Sigma), ROCK (AnaSpec) and actin, Alexa Fluor 488- or 594-conjugated Phalloidin (Molecular Probes); rat, rabbit and mouse IgGs (Jackson Labs); Alexa Fluor 488 and 555-conjugated anti-mouse, rat, and rabbit IgGs (Molecular Probes), HRP-conjugated rabbit and mouse secondary Abs (Amersham Pharmacia).

ROCK inhibitor was Y-27632 (40 μM; Calbiochem), and myosin inhibitor was Blebbistatin (50 mM); MEK-1 inhibitors were PD 98059 and U0126 (12.5 μM; BIOMOL).

Cell culture

The HMT3522 and MCF10A MECs and NIH 3T3 cells were maintained as described (Debnath et al., 2003; Wang et al., 1998; Yeung et al., 2005).

Mouse manipulations

FVB-TgN (MMTV-c-*myc*, *Her2/neu*, and H-*ras*) mice were maintained in accordance with the guidelines of Laboratory Animal Research at the University of Pennsylvania. Once tumors formed (12–24 weeks), mice were sacrificed, and the inguinal mammary glands were excised and analyzed. Tissues were fixed in 4% paraformaldehyde, and paraffin sections were stained with H&E for histopathological evaluation.

Gel manipulations

ECM-crosslinked PA gels were prepared and mechanically analyzed as described (Reinhart-King et al., 2003). For more details, see the Supplemental Experimental Procedures available with this article online.

Materials properties of tissues and natural gels

An electromechanical computer-controlled indenter comprised of a miniature linear stepper motor (minimal displacement 0.0032 mm), force transducer (load capacity 1.47 N), and a linear variable displacement transducer was used to measure the material stiffness of mammary tissue and ECM gels. The tangent elastic modulus of the unconfined stress-strain curve (slope) was calculated between 5% and 15% constant strain (Gefen et al., 2003).

tfm

Images of cells on PA gels containing fluorescent beads were collected before and after trypsinization using a Nikon Inverted Eclipse TE300 microscope and a Photometric Cool Snap HQ camera (Roper Scientific). TFMs were calculated based on differences in bead displacement induced by substrate deformation and relaxation using a software analysis program (Reinhart-King et al., 2003).

Shear force manipulations

Cells on FN-crosslinked PA (450 G′) gel-coated coverslips were subjected to a centrifugal shear force (room temperature [RT]) and analyzed for morphology, integrin adhesions, and FAK. Because the strain field increases with radius from the center of the disk according to the equation $\tau = 0.800r\sqrt{(\rho\mu\omega^3)}$, where τ is the shear stress exerted on a cell, ρ is the density, μ is the buffer viscosity, and ω is the rotational speed, the force applied to each cell was calculated based upon its radial position on the disk and the applied RPM. Cell attachment strength was assessed based upon the τ_{50}, which corresponds to the shear stress required to detach 50% of the adhered cells (Shi and Boettiger, 2003). For more details, see the Supplemental Experimental Procedures.

Immunofluorescence

Cells were extracted by CSK buffer and fixed or directly fixed using 2% paraformaldehyde (RT) or methanol (–20°C). Some cultures were embedded in sucrose and frozen in Tissue-Tek OCT compound, and 20 μm sections were immunostained. Paraffin-embedded tissue sections (4 μm) were subjected to antigen retrieval (citrate buffer) prior to immunostaining. All samples were incubated with primary mAb followed by Alexa-conjugated secondary Abs. Nuclei were counterstained with diaminophenylindole (DAPI; Sigma). Cells were visualized using a Bio-Rad MRC 1024 laser scanning confocal microscope attached to a Nikon Diaphot 200 microscope. Images were recorded at 120× magnification.

Morphometric analysis

Cell area was calculated by tracing phase images of fixed cells, and colony size was determined by tracing colony diameter of live colony images using a Nikon Inverted Eclipse TE300 microscope and a Photometric Cool Snap HQ camera (Roper Scientific) and ImagePro software (Yeung et al., 2005). To quantify integrin adhesion size, Z-stacked images of integrin adhesions were acquired using a Bio-Rad MRC 1024 confocal microscope, and images were processed with a computer-based analysis package, ImagePro (Zajaczkowski et al., 2003), and statistically analyzed using a two-tailed Student's t test.

Proliferation

Cell proliferation was measured by calculating the percent Ki67-labeled nuclei (Weaver et al., 2002).

Quantification of integrin activity and cell adhesion

Cell adhesion was assessed using a fluorescence attachment assay (Zahir et al., 2003), and integrin activity was quantified by immunoblotting (Tzima et al., 2001).

Immunoblot analysis

Equal RIPA or Laemmli lysate was separated on SDS-PAGE gels, immunoblotted, and detected with an ECL system (Amersham).

Vector description

Myc-tagged V14RhoA and EGFP-tagged N19RhoA in LZRS-IRES-blasticidin were used directly (Zahir et al., 2003). The constitutively active human β1 integrin glycan wedge mutant G429N in pEF1/V5-His has been characterized (Luo et al., 2004). V737N and G744N mutations were generated using the QuikChange Site-Directed Mutagenesis Kit (Stratagene) from the full-length human β1 integrin cDNA (gift of Z. Werb), and constructs were fused by PCR to EGFP at the C terminus or expressed bicistronically with EGFP in the Tet off system.

Ectopic gene expression

Retrovirus was produced in 293 or Phoenix ampho cells (G. Nolan), and cells were selected using G418, puromycin, or blasticidin. Transfections

with wild-type β1 in pcDNA 3.1, G429N β1 integrin in pEF1/V5-His, and EGFP in PRC CMV plasmid DNA were with Lipofectamine (Gibco BRL).

Rho GTPase activity

Cells were lysed in G protein buffer, and Rho GTPase activity was assayed using purified GST-Rhotekin and a Rhotekin pulldown assay (Tzima et al., 2001).

Supplemental data

The Supplemental Data include Supplemental Experimental Procedures, five supplemental figures, and enlargements of Figures 1D, 2D, 3B, and 4C and can be found with this article online at http://www.cancercell.org/cgi/content/full/8/3/241/DC1/.

Acknowledgments

We thank T. Springer and J. Takagi for the G429N β1 integrin mutant; Z. Werb for the β1 integrin construct; P. Marinkovich for the BM165 mAb; M. Schwartz for the GST-Rhotekin cDNA; D. Gasser and B. Alston-Mills for help with the mice; W. Lee and P. Janmey for sharing materials; L. Lynch for technical assistance; and R. Assoian for helpful comments. This work was supported by NIH grant CA078731 and DOD grants DAMD1701-1-0368, 1703-1-0496, and W81XWH-05-1-330 to V.M.W.; NIH grants HL57204 (to S.S.M.), GM57388 (to D.B.), BRP HL6438801A1 (to V.M.W. and D.A.H.), and T32HL00795404 (to N.Z. and K.R.J.); and DOD grants DAMD17-01-1-0367 and 17-03-1-0421 to J.N.L. and G.I.R.

Received: May 24, 2005
Revised: August 15, 2005
Accepted: August 24, 2005
Published: September 19, 2005

References

Akiri, G., Sabo, E., Dafni, H., Vadasz, Z., Kartvelishvily, Y., Gan, N., Kessler, O., Cohen, T., Resnick, M., Neeman, M., and Neufeld, G. (2003). Lysyl oxidase-related protein-1 promotes tumor fibrosis and tumor progression in vivo. Cancer Res. *63*, 1657–1666.

Arias-Salgado, E.G., Lizano, S., Sarkar, S., Brugge, J.S., Ginsberg, M.H., and Shattil, S.J. (2003). Src kinase activation by direct interaction with the integrin β cytoplasmic domain. Proc. Natl. Acad. Sci. USA *100*, 13298–13302.

Azar, F.S., Metaxas, D.N., and Schnall, M.D. (2001). A deformable finite element model of the breast for predicting mechanical deformations under external perturbations. Acad. Radiol. *8*, 965–975.

Beil, M., Micoulet, A., von Wichert, G., Paschke, S., Walther, P., Omary, M.B., Van Veldhoven, P.P., Gern, U., Wolff-Hieber, E., Eggermann, J., et al. (2003). Sphingosylphosphorylcholine regulates keratin network architecture and visco-elastic properties of human cancer cells. Nat. Cell Biol. *5*, 803–811.

Bershadsky, A.D., Balaban, N.Q., and Geiger, B. (2003). Adhesion-dependent cell mechanosensitivity. Annu. Rev. Cell Dev. Biol. *19*, 677–695.

Burridge, K., and Wennerberg, K. (2004). Rho and Rac take center stage. Cell *116*, 167–179.

Callister, W.D. (2000). Fundamentals of Materials Science and Engineering: An Interactive E-Text, Fifth Edition (Somerset, NJ: John Wiley & Sons, Inc.).

Chrzanowska-Wodnicka, M., and Burridge, K. (1996). Rho-stimulated contractility drives the formation of stress fibers and focal adhesions. J. Cell Biol. *133*, 1403–1415.

Colpaert, C., Vermeulen, P., Van Marck, E., and Dirix, L. (2001). The presence of a fibrotic focus is an independent predictor of early metastasis in lymph node-negative breast cancer patients. Am. J. Surg. Pathol. *25*, 1557–1558.

Croft, D.R., Sahai, E., Mavria, G., Li, S., Tsai, J., Lee, W.M., Marshall, C.J., and Olson, M.F. (2004). Conditional ROCK activation in vivo induces tumor cell dissemination and angiogenesis. Cancer Res. *64*, 8994–9001.

Debnath, J., Muthuswamy, S.K., and Brugge, J.S. (2003). Morphogenesis and oncogenesis of MCF-10A mammary epithelial acini grown in three-dimensional basement membrane cultures. Methods *30*, 256–268.

Delcommenne, M., and Streuli, C.H. (1995). Control of integrin expression by extracellular matrix. J. Biol. Chem. *270*, 26794–26801.

Engler, A.J., Griffin, M.A., Sen, S., Bonnemann, C.G., Sweeney, H.L., and Discher, D.E. (2004). Myotubes differentiate optimally on substrates with tissue-like stiffness: pathological implications for soft or stiff microenvironments. J. Cell Biol. *166*, 877–887.

Fritz, G., Just, I., and Kaina, B. (1999). Rho GTPases are over-expressed in human tumors. Int. J. Cancer *81*, 682–687.

Galbraith, C.G., Yamada, K.M., and Sheetz, M.P. (2002). The relationship between force and focal complex development. J. Cell Biol. *159*, 695–705.

Gefen, A., Gefen, N., Zhu, Q., Raghupathi, R., and Margulies, S.S. (2003). Age-dependent changes in material properties of the brain and braincase of the rat. J. Neurotrauma *20*, 1163–1177.

Guo, W., and Giancotti, F.G. (2004). Integrin signalling during tumour progression. Nat. Rev. Mol. Cell Biol. *5*, 816–826.

Huang, H., Kamm, R.D., and Lee, R.T. (2004). Cell mechanics and mechanotransduction: pathways, probes, and physiology. Am. J. Physiol. Cell Physiol. *287*, 1–11.

Keller, R., Davidson, L.A., and Shook, D.R. (2003). How we are shaped: the biomechanics of gastrulation. Differentiation *71*, 171–205.

Khaled, W., Reichling, S., Bruhns, O.T., Boese, H., Baumann, M., Monkman, G., Egersdoerfer, S., Klein, D., Tunayar, A., Freimuth, H., et al. (2004). Palpation imaging using a haptic system for virtual reality applications in medicine. Stud. Health Technol. Inform. *98*, 147–153.

Lark, A.L., Livasy, C.A., Dressler, L., Moore, D.T., Millikan, R.C., Geradts, J., Iacocca, M., Cowan, D., Little, D., Craven, R.J., and Cance, W. (2005). High focal adhesion kinase expression in invasive breast carcinomas is associated with an aggressive phenotype. Mod Pathol., in press. Published online April 29, 2005. 10.1038/modpathol.3800424.

Lee, J.W., and Juliano, R. (2004). Mitogenic signal transduction by integrin- and growth factor receptor-mediated pathways. Mol. Cells *17*, 188–202.

Li, R., Mitra, N., Gratkowski, H., Vilaire, G., Litvinov, R., Nagasami, C., Weisel, J.W., Lear, J.D., DeGrado, W.F., and Bennett, J.S. (2003). Activation of integrin αIIbβ3 by modulation of transmembrane helix associations. Science *300*, 795–798.

Liu, H., Radisky, D.C., Wang, F., and Bissell, M.J. (2004). Polarity and proliferation are controlled by distinct signaling pathways downstream of PI3-kinase in breast epithelial tumor cells. J. Cell Biol. *164*, 603–612.

Lo, C.M., Wang, H.B., Dembo, M., and Wang, Y.L. (2000). Cell movement is guided by the rigidity of the substrate. Biophys. J. *79*, 144–152.

Luo, B.H., Takagi, J., and Springer, T.A. (2004). Locking the β3 integrin I-like domain into high and low affinity conformations with disulfides. J. Biol. Chem. *279*, 10215–10221.

Luo, B.H., Carman, C.V., Takagi, J., and Springer, T.A. (2005). Disrupting integrin transmembrane domain heterodimerization increases ligand binding affinity, not valency or clustering. Proc. Natl. Acad. Sci. USA *102*, 3679–3684.

McLean, G.W., Komiyama, N.H., Serrels, B., Asano, H., Reynolds, L., Conti, F., Hodivala-Dilke, K., Metzger, D., Chambon, P., Grant, S.G., and Frame, M.C. (2004). Specific deletion of focal adhesion kinase suppresses tumor formation and blocks malignant progression. Genes Dev. *18*, 2998–3003.

Moore, K.A., Huang, S., Kong, Y., Sunday, M.E., and Ingber, D.E. (2002). Control of embryonic lung branching morphogenesis by the Rho activator, cytotoxic necrotizing factor 1. J. Surg. Res. *104*, 95–100.

Netti, P.A., Berk, D.A., Swartz, M.A., Grodzinsky, A.J., and Jain, R.K. (2000).

Role of extracellular matrix assembly in interstitial transport in solid tumors. Cancer Res. *60*, 2497–2503.

Nicolas, A., Geiger, B., and Safran, S.A. (2004). Cell mechanosensitivity controls the anisotropy of focal adhesions. Proc. Natl. Acad. Sci. USA *101*, 12520–12525.

O'Brien, L.E., Jou, T.S., Pollack, A.L., Zhang, Q., Hansen, S.H., Yurchenco, P., and Mostov, K.E. (2001). Rac1 orientates epithelial apical polarity through effects on basolateral laminin assembly. Nat. Cell Biol. *3*, 831–838.

O'Brien, L.E., Zegers, M.M., and Mostov, K.E. (2002). Opinion: Building epithelial architecture: insights from three-dimensional culture models. Nat. Rev. Mol. Cell Biol. *3*, 531–537.

Padera, T.P., Stoll, B.R., Tooredman, J.B., Capen, D., di Tomaso, E., and Jain, R.K. (2004). Pathology: cancer cells compress intratumour vessels. Nature *427*, 695.

Paszek, M.J., and Weaver, V.M. (2004). The tension mounts: mechanics meets morphogenesis and malignancy. J. Mammary Gland Biol. Neoplasia *9*, 325–342.

Reinhart-King, C.A., Dembo, M., and Hammer, D.A. (2003). Endothelial cell traction forces on RGD-derivatized polyacrylamide substrata. Langmuir *19*, 1573–1579.

Riveline, D., Zamir, E., Balaban, N.Q., Schwarz, U.S., Ishizaki, T., Narumiya, S., Kam, Z., Geiger, B., and Bershadsky, A.D. (2001). Focal contacts as mechanosensors: externally applied local mechanical force induces growth of focal contacts by an mDia1-dependent and ROCK-independent mechanism. J. Cell Biol. *153*, 1175–1186.

Roovers, K., and Assoian, R.K. (2003). Effects of rho kinase and actin stress fibers on sustained extracellular signal-regulated kinase activity and activation of G(1) phase cyclin-dependent kinases. Mol. Cell. Biol. *23*, 4283–4294.

Sahai, E., and Marshall, C.J. (2002). ROCK and Dia have opposing effects on adherens junctions downstream of Rho. Nat. Cell Biol. *4*, 408–415.

Sahai, E., Olson, M.F., and Marshall, C.J. (2001). Cross-talk between Ras and Rho signalling pathways in transformation favours proliferation and increased motility. EMBO J. *20*, 755–766.

Shi, Q., and Boettiger, D. (2003). A novel mode for integrin-mediated signaling: tethering is required for phosphorylation of FAK Y397. Mol. Biol. Cell *14*, 4306–4315.

Tzima, E., del Pozo, M.A., Shattil, S.J., Chien, S., and Schwartz, M.A. (2001). Activation of integrins in endothelial cells by fluid shear stress mediates Rho-dependent cytoskeletal alignment. EMBO J. *20*, 4639–4647.

Vial, E., Sahai, E., and Marshall, C.J. (2003). ERK-MAPK signaling coordinately regulates activity of Rac1 and RhoA for tumor cell motility. Cancer Cell *4*, 67–79.

Wang, F., Weaver, V.M., Petersen, O.W., Larabell, C.A., Dedhar, S., Briand, P., Lupu, R., and Bissell, M.J. (1998). Reciprocal interactions between β1-integrin and epidermal growth factor receptor in three-dimensional basement membrane breast cultures: a different perspective in epithelial biology. Proc. Natl. Acad. Sci. USA *95*, 14821–14826.

Wang, H.B., Dembo, M., and Wang, Y.L. (2000). Substrate flexibility regulates growth and apoptosis of normal but not transformed cells. Am. J. Physiol. Cell Physiol. *279*, C1345–C1350.

Weaver, V.M., Lelievre, S., Lakins, J.N., Chrenek, M.A., Jones, J.C., Giancotti, F., Werb, Z., and Bissell, M.J. (2002). β4 integrin-dependent formation of polarized three-dimensional architecture confers resistance to apoptosis in normal and malignant mammary epithelium. Cancer Cell *2*, 205–216.

White, D.E., Kurpios, N.A., Zuo, D., Hassell, J.A., Blaess, S., Mueller, U., and Muller, W.J. (2004). Targeted disruption of β1-integrin in a transgenic mouse model of human breast cancer reveals an essential role in mammary tumor induction. Cancer Cell *6*, 159–170.

Wozniak, M.A., Desai, R., Solski, P.A., Der, C.J., and Keely, P.J. (2003). ROCK-generated contractility regulates breast epithelial cell differentiation in response to the physical properties of a three-dimensional collagen matrix. J. Cell Biol. *163*, 583–595.

Yeung, T., Georges, P.C., Flanagan, L.A., Marg, B., Ortiz, M., Funaki, M., Zahir, N., Ming, W., Weaver, V., and Janmey, P.A. (2005). Effects of substrate stiffness on cell morphology, cytoskeletal structure, and adhesion. Cell Motil. Cytoskeleton *60*, 24–34.

Zahir, N., Lakins, J.N., Russell, A., Ming, W., Chatterjee, C., Rozenberg, G.I., Marinkovich, M.P., and Weaver, V.M. (2003). Autocrine laminin-5 ligates α6β4 integrin and activates RAC and NFκB to mediate anchorage-independent survival of mammary tumors. J. Cell Biol. *163*, 1397–1407.

Zajaczkowski, M.B., Cukierman, E., Galbraith, C.G., and Yamada, K.M. (2003). Cell-matrix adhesions on poly(vinyl alcohol) hydrogels. Tissue Eng. *9*, 525–533.

Zhong, C., Kinch, M.S., and Burridge, K. (1997). Rho-stimulated contractility contributes to the fibroblastic phenotype of Ras-transformed epithelial cells. Mol. Biol. Cell *8*, 2329–2344.